Complementary Observer for Body Segments Motion Capturing by Inertial and Magnetic Sensors

Hassen Fourati, Noureddine Manamanni, Lissan Afilal, Yves Handrich

A Complementary Sliding Mode Observer Approach for Motions Human Body Segments Capturing by Means of Wearable Inertial and Magnetic MEMS Sensors Assembly

Hassen Fourati, *Student, IEEE,* Noureddine Manamanni*, *Member, IEEE,* Lissan Afilal, Yves Handrich

***Abstract*—The aim of the paper is to develop and to validate an estimation approach of human body segments motion (also known as attitude). The challenge of the proposed approach is that it uses only a wearable Inertial Measurement Unit (IMU) and without resorting to GPS data. This unit consists of Micro-Electro-Mechanical-Systems (MEMS) sensors as a 3-axis accelerometer, a 3-axis magnetometer and a 3-axis gyroscope. Based on these sensors, the final objective is to design a low-cost and lightweight prototype and easy to use by persons. The prototype can then be used in many applications as ambulatory monitoring of human body motion in order to evaluate the corresponding mechanical work. To reach this goal, a quaternion-based Complementary Sliding Mode Observer (CSMO) is designed with a multiplicative quaternion correction technique. This algorithm will continuously correct the quaternion estimates obtained by integration of the angular velocity. The correction is performed using a quaternion obtained from the accelerometer and the magnetometer data fusion based on the Levenberg Marquardt Algorithm (LMA). The efficiency of the CSMO is illustrated through simulation tests using a theoretical example. Moreover, a set of experiments is performed on a robot and human limbs motion through sensor measurements provided by an IMU.**

***Index Terms*—Motion capturing, human limbs motion sensing, Complementary Sliding Mode Observer, Inertial Unit, wearable inertial/magnetic MEMS sensors, quaternion, rehabilitation.**

I. Introduction

The determination of moving objects orientation is involved in several fields: among them, of interest here, ambulatory human motion tracking and analysis [1]. Moreover, the current information of orientation still one of the central assessment tools in many related application as stroke rehabilitation to help patients to restore motor functions of the affected limbs [2], gait analysis [3], monitoring of daily living [4], and measurement of neurological disorders in medicine [5].

A literature survey shows that there are currently several fundamental technologies embedded within human movement tracking systems, which consistently update spatio-temporal information with regard to human motion. These technologies can contain mechanical tracking, electromagnetic tracking, acoustic tracking, optical tracking, and inertial/magnetic tracking [1]. Among these techniques, inertial/magnetic tracking technology has currently attracted many interests since such method is free of most of the problems occurring with the other technologies. An inertial/magnetic tracking system uses a combination of accelerometers, rate gyros, and magnetic sensors and is suitable for ambulatory measurement of human body segments orientation without restrictions [6]. There is no inherent latency associated with inertial/magnetic sensing and all delays are due to data transmission and processing. Another benefit with inertial/magnetic sensing is its sourceless, whereas electromagnetic, acoustic, and optic devices require emissions from source to track objects.

Nowadays, due to the recent technological advances of MEMS, inertial and magnetic sensors have become generally available with a low cost, small size, light weight and low energy consumption. Consequently, human motion estimation can be tracked continuously outside of a laboratory with quite smaller and ambulatory measurement system. Each of these sensors has different advantages and disadvantages. Accelerometers measure acceleration and gravity [7] and can be used as an inclinometer for movements in which the acceleration can be neglected with respect to the gravity [8]. However, this way to do leads to unacceptable errors in dynamic human motion. Gyroscopes measure angular velocity and can be used to estimate a change in orientation. The drawback of gyroscopes is that the estimation of orientation change is prone to integration drift [9]. Magnetometers are used to measure the local earth magnetic field vector. This provides additional information about orientation [10].

Several advanced signal processing fusion approaches for integrating the sensors described above to estimate human segments orientation have been proposed in order to overcome the drawbacks of the separate sensors and to improve the performance of existing sensing hardware. The basic idea behind complementary filtering is that orientation drift errors resulting from gyro output errors can be bounded by aiding the gyros with additional sensors, the information from which allows correcting the gyro orientation solution. In [11], the authors combined sensors such as 3-axis accelerometer and 3-axis magnetometer to measure the body orientation. A 3-axis

Manuscript received October 30, 2010.

H. Fourati, N. Manamanni and L. Afilal are with CReSTIC-URCA, Reims Champagne Ardenne University, UFR SEN, Moulin de la Housse, EA 3804, BP 1039, 51687, Reims, Cedex 02, France (* Corresponding author. Phone: +33326918386; Fax: +33326913106; e-mail: noureddine.manamanni@univ-reims.fr).

Y. Handrich and H. Fourati are with IPHC-DEPE-CNRS, Strasbourg University, 23 rue Becquerel, 67087, Strasbourg, Cedex 2, France.

gyroscope and 3-axis accelerometer were applied by [12] and the proposed works are developed based on a Kalman filter for measuring orientation. The main idea in [3] concerns the use of the cyclical nature of human gait to provide attitude estimation based on angular velocity rate and acceleration measurements. The change in orientation obtained using gyroscopes was fused with the inclination measured by the accelerometers, yielding an inclination estimate that was sufficiently accurate even in the presence of accelerations.

The main purpose in [13] deals with the addition of magnetometers to gyroscopes and accelerometers to overcome this problem. A linear Kalman Filter was designed to process the sensor signals to estimate desired sensing variables of gravity and magnetic field, and further yields orientation of the body segment. Heading errors due to magnetic field disturbance can be effectively rejected by an adequate model-based sensor fusion [14]. This triad of sensors is used also in [15], [16] to develop an Extended Kalman Filter (EKF). Another method to obtain kinematics between 2 body segments is to estimate the orientations of each segment using a multiple sensor system and to use anatomical constraints to link the different segments [2], [3].

Quaternion has been the subject of studies in many attitude and motion capturing systems using various filtering theories. Due to the unconventional nature of quaternion kinematics, filter models have been synthesized in two different ways related to the objectives, the formulation of the measurement error vector and the update of the state estimates. The first way is based on additive quaternion correction [15], [17]. This approach is easy to implement but it is considered as localized approximation since it is valid only for small attitude changes. The second way uses multiplicative quaternion correction [18], [19] and can be applied for larger attitude maneuvers.

In this paper, an alternative sensing method for the human limbs motion estimation is developed then validated. This approach is based on a fusion technique of inertial and magnetic sensors. The main goal is to use the obtained results to monitor human movements during rehabilitation exercises. One of the interests of this work is also to look for the ambulatory monitoring of the elderly movements. Hence, we propose a robust method recovering the full attitude represented by a quaternion and which represents the rigid body motion. The main idea is to use a Complementary Sliding Mode Observer (CSMO) instead of Extended Kalman Filter that presents some drawbacks such as the difficulty to guarantee the global convergence of the filter due to the linear approximation of the nonlinear process model [20].

The proposed CSMO exploits the multiplicative quaternion correction technique to recover the full rigid body orientation. The designed observer is fed with inertial and magnetic measurements and takes into account the complementary spectra of the signals. In fact, the estimation algorithm idea uses 3-axis gyroscope measurements to derive the attitude (strap-down system). The correction was performed using a quaternion continuously derived from a 3-axis accelerometer and a 3-axis magnetometer data fusion method that is based on Levenberg Marquardt Algorithm (LMA). This reduces the integration drift that originates from the angular velocity.

This paper is organized as follows: section II describes the problem statement and our motivations. Section III presents the physical system including the rigid body kinematic equation and the design model. Section IV details the structure of the proposed CSMO for motion estimation. In section V, some simulation tests are presented to illustrate the performance of the proposed approach. Experimental trials are designed on a robot and a human subject in section VI to demonstrate the efficiency of the developed filtering technique. Finally some conclusions are given in section VII.

II. Motivation and problem definition

The main contribution of the performed work in this paper is to propose available approach to estimate the movement patterns (attitude or orientation) of human body segments. Each segment can be represented by a rigid body. Generally, the body attitude is an essential quantity that serves as tool, for biologists, to estimate the power transferred between the human body and the environment at any time and the energy expenditure. This is of great interest in a number of applications, including sport (stride analysis), physical labor, fitness management and rehabilitation [18], [21].

Indeed, we have conducted some researches for human motion tracking with the use the minimum of wearable sensors assembly [20]. Since inertial and magnetic devices have become generally available due to the recent technological advances of MEMS [22], human movement can be measured continuously outside a specialized laboratory with ambulatory systems. Then, the use of Inertial Measurement Unit that contains a 3-axis accelerometer, a 3-axis magnetometer and a 3-axis gyroscope is suitable for the considered application related to the human motion tracking (see Fig. 1).

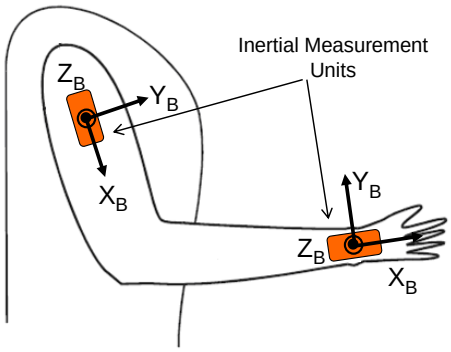

Fig. 1. Schematic representation of the body segments-mounted sensing unit for motion estimation

Since each sensor shows some advantages and drawbacks, the key of the work is how to combine these three data to improve the quality of the motion reconstruction.

III. The physical system

A. Rigid body kinematic motion equation

The motion of a rigid body can be described by the following attitude kinematic differential equation [23]:

$$\frac{\partial q}{\partial t} = \frac{1}{2}\bar{\omega}_g \otimes q \qquad (1)$$

where:

- $q = \begin{bmatrix} q_0 & q_{vect}^T \end{bmatrix}^T$ is the unit quaternion that denotes the mathematical representation of the rigid body attitude between two frames: body-fixed frame B and Earth-fixed frame N. Note that $q_{vect} = \begin{bmatrix} q_1 & q_2 & q_3 \end{bmatrix}^T$ represents the vector part of q. It is customary to use quaternions instead of Euler angles since they provide a global parameterization of the body orientation, and are well-suited for calculations and computer simulations. More details about quaternion and the used frames are presented in appendixes A and B.
- $\bar{\omega}_g = \begin{bmatrix} 0 & \omega_g \end{bmatrix}^T$ is the quaternion form of the angular velocity vector $\omega_g = \begin{bmatrix} \omega_{gx} & \omega_{gy} & \omega_{gz} \end{bmatrix}^T$ expressed in B. Recall that ω_g is measured by a 3-axis gyroscope and can be often corrupted with noises and bias $\gamma(t)$ [20].
- The operator $\otimes$ represents the quaternion product and is defined in appendix A (equation (25)).

Equation (1) describes the time rate of change of the attitude, expressed in a quaternion term q, as a result of the rigid body angular rates measured by the gyroscope.
Now, including gyroscope disturbances and using the quaternion product $\otimes$, (1) can be written such as:

$$\frac{\partial q}{\partial t} = \frac{1}{2}\begin{bmatrix} -q_{vect}^T \\ I_{3\times 3}\, q_0 + \begin{bmatrix} q_{vect}^{\times} \end{bmatrix} \end{bmatrix} \omega_g + w(t) \tag{2}$$

where $q_{vect} = \begin{bmatrix} q_1 & q_2 & q_3 \end{bmatrix}^T$ and $\begin{bmatrix} q_{vect}^{\times} \end{bmatrix}$ represents the skew-symmetric matrix defined as [24]:

$$\begin{bmatrix} q_{vect}^{\times} \end{bmatrix} = \begin{bmatrix} q_1 \\ q_2 \\ q_3 \end{bmatrix}^{\times} = \begin{bmatrix} 0 & -q_3 & q_2 \\ q_3 & 0 & -q_1 \\ -q_2 & q_1 & 0 \end{bmatrix} \tag{3}$$

and $I_{3\times 3}$ is the identity matrix of dimension 3.

B. The design model

Let us consider the following nonlinear system model (Σ) composed of (2) with the output y that represents the linear measurement model:

$$(\Sigma): \begin{cases} \dfrac{\partial q}{\partial t} = \dfrac{1}{2}\begin{bmatrix} -q_{vect}^T \\ I_{3\times 3}\, q_0 + \begin{bmatrix} q_{vect}^{\times} \end{bmatrix} \end{bmatrix} \omega_g + \gamma(t) \\ y = Cq + v \end{cases} \tag{4}$$

where q represents the quaternion vector. $C = I_{4\times 4}$ and v represents the noises vector. Then, the linear measurement model y is taken as follows $y = q_m \in \Re^{4\times 1}$. Note that the rigid body quaternion measurements q_m may be determined from a 3-axis accelerometer and a 3-axis magnetometer data fusion method (see the next part for more details).

By considering the rigid body kinematic equation and the linear measurement model y, the proposed system (Σ) can take advantage from the good short term precision given by the rate gyros integration and the reliable long term accuracy provided by accelerometers and magnetometers measurements fusion [20] which leads to improve the quaternion estimation.

C. Quaternion q_m calculation from accelerometer and magnetometer measurements

The problem of optimal attitude determination algorithm using two vectors (or more), known in a fixed frame (vector observations) and measured in a mobile frame is called in the literature *Wahba's problem* [25]. In the present case, the 3-axis magnetometer is a sensor that provides the direction of the Earth's magnetic field h in the body frame B such as:

$$h = \begin{bmatrix} h_x & h_y & h_z \end{bmatrix}^T = M_N^B(q)\, m + \delta_h \tag{5}$$

where $M_N^B(q)$ is the rotation matrix that transforms the vector m to the vector h:

$$M_N^B(q) = \begin{bmatrix} 2q_0^2 + 2q_1^2 - 1 & 2(q_1q_2 + q_0q_3) & 2(q_1q_3 - q_0q_2) \\ 2(q_1q_2 - q_0q_3) & 2q_0^2 + 2q_2^2 - 1 & 2(q_0q_1 + q_2q_3) \\ 2(q_0q_2 + q_1q_3) & 2(q_2q_3 - q_0q_1) & 2q_0^2 + 2q_3^2 - 1 \end{bmatrix} \tag{6}$$

and $\delta_h \in \Re^3$ is a vector of zero-mean white Gaussian noise.
m represents the magnetic field vector measured in the Earth-fixed frame N and can be represented such as:

$$m = \begin{bmatrix} m_x & 0 & m_z \end{bmatrix}^T = \begin{bmatrix} \|m\|\cos(\theta) & 0 & \|m\|\sin(\theta) \end{bmatrix}^T \tag{7}$$

The theoretical model of the magnetic field nearest to reality considers this vector with an inclination angle $\theta = 60°$ and a norm vector $\|m\| = 0.5$ Gauss [26]. The quantity h is locally constant in the fixed frame N and can be represented by the vector m which denotes ***the first vector observation***.

The 3-axis accelerometer measures the specific force f in the body frame B as follows [7]:

$$f = \begin{bmatrix} f_x & f_y & f_z \end{bmatrix}^T = M_N^B(q)\left[a + g\right] + \delta_f \tag{8}$$

where $g = \begin{bmatrix} 0 & 0 & 9.81 \end{bmatrix}^T$ represents the gravity vector and $a = \begin{bmatrix} a_x & a_y & a_z \end{bmatrix}$ denotes the inertial acceleration of the body, expressed in the Earth frame N [27]. The rotation matrix $M_N^B(q)$ is as expressed in (6). $\delta_f \in \Re^3$ is a vector of zero-mean white Gaussian noise. For sufficiently low frequency bandwidths, the gravitational field g dominates the accelerometer measurements f $\left(\|a\|_2 \ll \|g\|_2\right)$, as discussed in [17]. In this case, the quantity g is also constant in the Earth frame N and could provide ***the second vector observation***.

For this purpose, a Levenberg Marquardt Algorithm (LMA) is proposed to recover the optimal attitude, expressed in quaternion term, by using 3-axis accelerometer and 3-axis

magnetometer readings [28]. The LMA outperforms the Gauss-Newton Algorithm (G.N.A) and the method of gradient descent. It is more robust than G.N.A, which means that in many cases it finds a solution even if it starts very far of the final minimum [29]. The LMA is an estimator that uses the Earth's magnetic field m and the gravity vector g as vector observations and the measurements f and h to deduce the attitude q_m. It is based on the followings steps [30]:

1) Measure accelerometer and magnetometer readings f and h, respectively.
2) Calculate $\hat{f}^N = \hat{q} \otimes f \otimes \bar{\hat{q}}$ and do the same for $\hat{h}^N$. Note that $\hat{f}^N$ and $\hat{h}^N$ represent the estimated acceleration and magnetic field values in the Earth-fixed frame N.
   Note also that $\bar{\hat{q}} = \begin{bmatrix} \hat{q}_0 & -\hat{q}_1 & -\hat{q}_2 & -\hat{q}_3 \end{bmatrix}^T$ represents the quaternion inverse of $\hat{q}$.
3) Calculate the navigation error $\partial f = g - \hat{f}^N$ and do the same for $\partial h = m - \hat{h}^N$ in order to form $z = \begin{bmatrix} \partial h & \partial f \end{bmatrix}^T$.
4) Calculate the Jacobian matrix:

$$J = -2 \begin{bmatrix} \begin{bmatrix} \begin{bmatrix} \hat{h}^N \end{bmatrix}^{\times} \end{bmatrix}^T & \begin{bmatrix} \begin{bmatrix} \hat{f}^N \end{bmatrix}^{\times} \end{bmatrix}^T \end{bmatrix}^T$$

5) Calculate the pseudo-inverse $O^* = \left[J^T J + \lambda I_{3\times 3} \right]^{-1} J^T$.
6) Calculate the quaternion error such as: $q_{er}(t) = \alpha O^* z$. α is a smooth parameter chosen between 0 and 1 [25].
7) Calculate q_m such as: $q_m(t) = \hat{q}(t) \otimes \begin{bmatrix} 1 & q_{er}(t) \end{bmatrix}^T$. $\hat{q}(t)$ is estimated at each step by the observer that we will present in the next section.

It is important to note that this algorithm is limited to the static or quasi-static situations (weak linear acceleration) [25]. Therefore, the values of q_m are disturbed in dynamic situations (high inertial acceleration periods). In this paper, the introduction of the term q_m in the system (4) aims to take advantage from the reliable long term accuracy provided by accelerometers and magnetometers measurements and the good short term precision given by rate gyros integration.

IV. 3-AXIS INERTIAL/MAGNETIC SENSORS PACKAGE FOR HUMAN MOTION ESTIMATION: COMPLEMENTARY SLIDING MODE OBSERVER APPROACH

In this section, the objective is to design an attitude estimation algorithm based on inertial and magnetic MEMS sensors. The application in mind is related to the human limbs motion estimation.

By considering the rigid body kinematic model, a Complementary Sliding Mode Observer (CSMO) is proposed in order to take advantage from the good short term precision given by rate gyros integration and the reliable long term accuracy provided by accelerometers and magnetometers measurements. This leads to better attitude estimates [17].

A. Observer design

The main emphasis of the proposed observer is based on the use of the multiplicative correction technique [31] which can be written as follows:

$$q' = \delta q \otimes q \tag{9}$$

Quaternion multiplication is used in (9) to correct and update the quaternion calculation. δq is the correction term which is a function of the measurement error. This technique is more convenient for the transition between two quaternions and can be applied for larger attitude motions [18].
To perform the quaternion estimates update, (9) can be transformed into the following form:

$$\hat{q}^+ = \delta \hat{q}^+ \otimes \hat{q}^- \tag{10}$$

where $\hat{q}^+$ and $\hat{q}^-$ represent the post and pre-update values of the quaternion estimates, respectively.

Finally, the CSMO for the system (Σ) in (4) can be designed based on (10). Generally, the choice of the sliding manifold is usually based on the state estimation error [32]. Thus, we choose the error quaternion as the sliding manifold. The proposed observer is given as follows:

$$CSMO: \begin{cases} \dot{\hat{q}} = \begin{bmatrix} \dot{\hat{q}}_0 \\ \dot{\hat{q}}_1 \\ \dot{\hat{q}}_2 \\ \dot{\hat{q}}_3 \end{bmatrix} = \delta_{K_1} \otimes \delta_{K_2} \otimes \begin{pmatrix} \frac{1}{2} \begin{bmatrix} -\hat{q}_{vect}^T \\ I_{3\times 3}\hat{q}_0 + \begin{bmatrix} \hat{q}_{vect}^{\times} \end{bmatrix} \end{bmatrix} \begin{bmatrix} \omega_{gx} \\ \omega_{gy} \\ \omega_{gz} \end{bmatrix} + \gamma(t) \end{pmatrix} \end{cases} \tag{11}$$

where $\hat{q}$ is the estimated quaternion at time t and $\begin{bmatrix} \hat{q}_{vect}^{\times} \end{bmatrix}$ is defined as in (3). δ_{K_1} represents the switching correction term and δ_{K_2} is the linear correction term. In order to perform the quaternion multiplication, each correction term should be converted into a quaternion. This conversion is obtained using the forced normalization method given in [33]. δ_{K_1} and δ_{K_2} are computed such as follows:

$$\delta_{K_1} = \frac{1}{\|\chi_1\|}\chi_1 \quad ; \quad \delta_{K_2} = \frac{1}{\|\chi_2\|}\chi_2 \tag{12}$$

where

$$\chi_1 = K_1 \begin{bmatrix} 1 & sat\left[\frac{q_{e,vect}}{\rho} \right] \end{bmatrix}^T \; ; \; \chi_2 = K_2 \begin{bmatrix} 1 & q_{e,vect} \end{bmatrix}^T \tag{13}$$

with

$$K_1 = \begin{bmatrix} 1 & 0 & 0 & 0 \\ 0 & k_1 & 0 & 0 \\ 0 & 0 & k_2 & 0 \\ 0 & 0 & 0 & k_3 \end{bmatrix} ; \; K_2 = \begin{bmatrix} 1 & 0 & 0 & 0 \\ 0 & k_4 & 0 & 0 \\ 0 & 0 & k_5 & 0 \\ 0 & 0 & 0 & k_6 \end{bmatrix} \tag{14}$$

Note that $q_{e,vect}$ in (13) represents the imaginary vector of the error quaternion q_e. q_e measures the discrepancy between the complementary estimated quaternion $\bar{\hat{q}} = \begin{bmatrix} \hat{q}_0 & -\hat{q}_1 & -\hat{q}_2 & -\hat{q}_3 \end{bmatrix}^T$ and the measured attitude q_m (obtained from LMA), that is:

$$q_e = q_m \otimes \bar{\hat{q}} = \begin{bmatrix} q_{e0} & q_{e,vect} \end{bmatrix}^T \quad (15)$$

The scalar parts of χ_1 and χ_2 are chosen very close to unit since the incremental quaternion corresponds to a small angle rotation [31]. The saturation function sat in (13) is used to avoid the high frequency chattering behavior around the sliding surface [32]:

$$sat\left[\frac{q_{e,vect}}{\rho}\right] = \begin{cases} 1 & q_{e,vect} \le \rho \\ \dfrac{q_{e,vect}}{\rho} & \left|q_{e,vect}\right| \le \left|\rho\right| \\ -1 & q_{e,vect} \ge \rho \end{cases} \quad (16)$$

The parameter ρ is the sliding surface boundary layer. It determines the sliding behavior in the vicinity of $q_{e,vect} = 0$. To preserve the unit quaternion norm, the estimated quaternion $\hat{q}$ in (11) must be normalized to avoid a divergence caused by round-off errors. Normalization is obtained such as [34]:

$$\hat{q}_{norm} = \frac{\hat{q}}{\left\|\hat{q}\right\|} \quad (17)$$

Finally, Fig. 2 illustrates the scheme of the proposed CSMO.

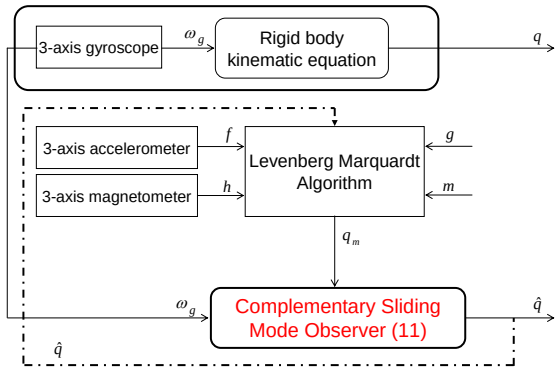

Fig.2. Scheme of the estimation algorithm

B. *Performance analysis of the designed observer*

A frequency analysis of inertial and magnetic sensors shows that signals coming from the accelerometer-magnetometer pair and signals from the gyroscope have a complementary frequency spectrum [20]. Therefore, the resulting structure of the proposed CSMO in (11) blends the low frequency region (low bandwidth) of the accelerometer and magnetometer data, where the attitude is typically more accurate, with the high frequency region (high bandwidth) of the gyroscope data, where the integration of the angular velocity yields better attitude estimates. The proposed observer is derived from the complementary filtering theory [35]. It explores the sensor redundancy to reject measurement disturbances in complementary frequency regions without distorting the signal. If the measurements have complementary spectral characteristics, transfer functions may be chosen in such way as to minimize the estimation error [19]. The general requirement is that one of the transfer functions complements the sum of the others. Thus for n measurements of a signal:

$$1 - T_1(s) - T_2(s) - \ldots - T_{n-1}(s) = T_n(s) \quad (18)$$

where s is the Laplace operator.

To study the performance of the CSMO, let us show the transform domain block diagram of the linearized quaternion observer (see Fig. 3). This diagram is obtained from Fig. 2.

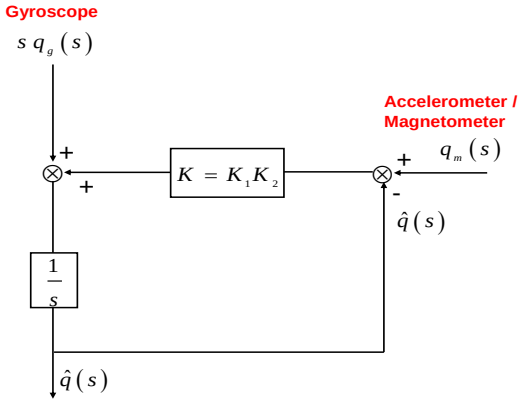

Fig. 3. Block diagram of the transform domain (Laplace) of the linearized quaternion estimation observer

Let the Laplace transform of the quaternion q_m (obtained from accelerometer and magnetometer readings fusion) be $q_m(s)$, while $q_g(s)$ is the quaternion obtained by integrating gyroscope signals and $sq_g(s)$ is the Laplace transform of $\dot{q}$ in (2). Note that the accelerometer measures both gravitational and linear accelerations and the gyroscope suffers from bias. Therefore, $q_m(s)$ and $q_g(s)$ are both disturbed. From Fig. 3, the filter transfer function $F_1(s)$ based on accelerometer and magnetometer inputs is given by:

$$F_1(s) = \frac{\hat{q}(s)}{q_m(s)} = \frac{Ks^{-1}}{1 + Ks^{-1}} = \frac{K}{s + K} \quad (19)$$

Note that equation (19) has the form of first-order low-pass filter which proves that the perturbation effects due to high frequency components of accelerometer signal (linear acceleration) are filtered from $q_m(s)$.

The gain K can be written such as $K = K_1 K_2$, where K_1 and K_2 are given in equation (14).

Similarly, from Fig. 3, the filter transfer function based on gyroscope inputs can be written such as:

$$F_2(s) = \frac{\hat{q}(s)}{q_g(s)} = \frac{1}{1 + Ks^{-1}} = \frac{s}{s + K} \quad (20)$$

Note that (20) has the form of first-order high-pass filter. The gyroscope measurements are high-pass filtered with respect to the output $\hat{q}(s)$. So, the perturbations due to low frequency components of gyroscope signal (the noises and biases) are filtered from $q_g(s)$.

Finally, (18) can be verified:

$$\frac{\hat{q}(s)}{q_m(s)} + \frac{\hat{q}(s)}{q_g(s)} = \frac{K}{s + K} + \frac{s}{s + K} = 1 \quad (21)$$

Note that (21) confirms the complementary aspect of the CSMO. The global transfer function of the observer is:

$$\hat{q}(s) = \left(\frac{K}{s+K}\right) q_m(s) + \left(\frac{s}{s+K}\right) q_g(s) \qquad (22)$$

We conclude from (22) that the CSMO blends a low-pass filtering on the signals from the accelerometer/magnetometer, and a high-pass filtering on the signals from the gyroscope.

V. SIMULATIONS RESULTS

This section aims to illustrate the performance of the CSMO proposed in (4) to estimate the rigid body attitude based on inertial and magnetic measurements. Some numerical simulations were carried out according to the conditions of our application on human limbs. Therefore, one considers a triad of sensors composed of a 3-axis accelerometer, a 3 axis magnetometer and a 3-axis gyroscope that is attached to a body segment (see Fig. 4). The instrument axes are nominally aligned with the body-platform axes.

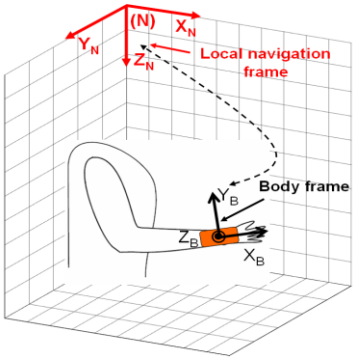

Fig. 4. Simulation using a theoretical representation of the final application

The simulations under *Matlab* begin with the generation of theoretical measurements of angular velocity, specific force and magnetic field taken respectively from gyroscope, accelerometer and magnetometer, during the human's segment motion (see Fig. 5). We consider an attitude variation example taken from angular velocity data (see Table I) over 60sec. Then, the kinematic equation (2) is solved to obtain the continuous time motion in quaternion representation using the theoretical angular velocity measurements. The obtained quaternion is used as a reference to compare it with the estimated quaternion from the CSMO.

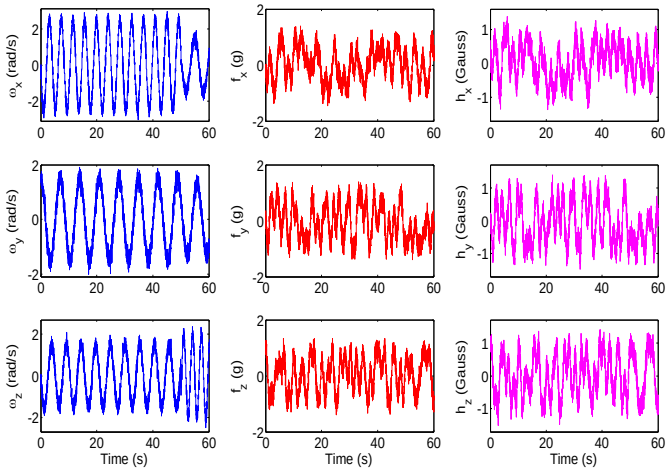

Fig. 5. Measurements taken during the human's segment theoretical motion

To represent the sensor imperfections, an additional random zero-mean white Gaussian noise was considered for all measurements (see Table II). The sampling rate was chosen as 100Hz for all measurements. The boundary layer thickness is set to $\delta = 3.10^{-4}$. The constants in the observer gains K_1 and K_2 (equation (14)) that guarantee convergent estimates, are set according to the sensor noise levels and sampling rate such as : $k_1 = k_2 = k_3 = 10^{-3}$ and $k_4 = k_5 = k_6 = 9.10^{-4}$.

TABLE I
THEORETICAL ANGULAR VELOCITY VALUES

Time	Angular velocity
$t \le 15\text{sec}$	$\omega_x(t) = -2.5\sin(1.5t)$ $\omega_y(t) = 1.5\cos(0.9t)$ $\omega_z(t) = -1.5\sin(1.2t)$
$15\text{sec} < t \le 30\,\text{sec}$	$\omega_x(t) = -1.5\sin(1.5t)$ $\omega_y(t) = 1.3\cos(1.3t)$ $\omega_z(t) = -2\sin(2t)$
$30\text{sec} < t \le 45\,\text{sec}$	$\omega_x(t) = -2.5\sin(1.5t)$ $\omega_y(t) = 1.5\cos(0.9t)$ $\omega_z(t) = -1.5\sin(1.2t)$
$45\text{sec} < t \le 60\,\text{sec}$	$\omega_x(t) = -1.5\sin(-1.5t)$ $\omega_y(t) = 1.3\cos(1.3t)$ $\omega_z(t) = -2\sin(2t)$

TABLE II
CHARACTERISTICS OF THE VARIOUS NOISES FOR THE SENSORS MEASUREMENTS

Sensors	Parameters	Standard deviations	Units
Accelerometer	δ_f	0.4	m/s^2
Magnetometer	δ_h	0.4	$Gauss$
Gyroscope	δ_g	0.4	rad/s

In this set of simulations, the theoretical components of the quaternion q are initialized with different random values as well as those estimated from the CSMO. These conditions are given such as: $q(t_0) = [1 \quad 0 \quad 0 \quad 0]^T$; $\hat{q}(t_0) = [0.2 \quad 0.5 \quad 0.7 \quad 0.3]^T$.

Note that this choice allows us to illustrate the convergence of the observer even though it was initialized far from the actual states. In order to evaluate the overall performance of the attitude estimation, we plotted the time history evolution of the estimation errors on the quaternion. Fig. 6 depicts the convergence of these errors towards zero during the simulated motion. For more clarity, two scales are used, one for periods between 0 and 5sec and another for periods lasting longer than 5sec. This zoom illustrates the convergence behavior early in the time course and shows the precision obtained after convergence as clearly as possible. Despite the fact that the CSMO and the theoretical model of the quaternion were initialized with different initial conditions, one can note that the estimated quaternion converges towards the theoretical values. The same performance was obtained when using different sets of initial conditions. The obtained results in Fig. 6 represent Euler angles errors around 3°.

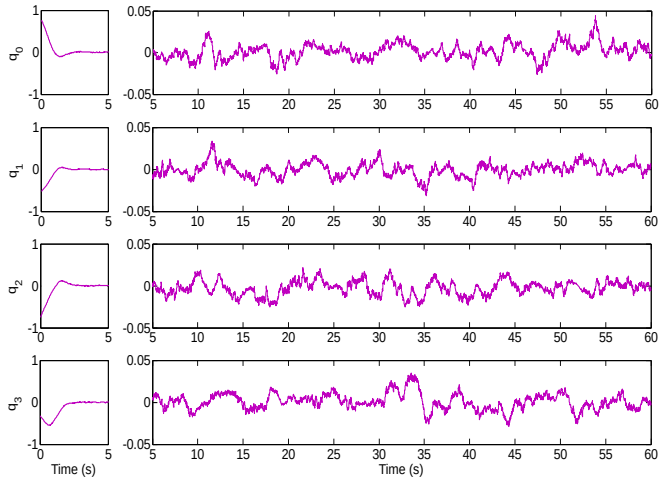

Fig. 6. Quaternion estimation errors using the CSMO (with a zoom between 5 and 60sec)

The observer copes well with the large noises introduced in the 3-axis gyroscope, the 3-axis accelerometer and the 3-axis magnetometer measurements.

In order to show the improvements made by the CSMO compared to the only use of the Levenberg Marquardt Algorithm, we depict in Fig. 7 the quaternion estimation errors resulting from the LMA. It is important to note that the rate of errors committed by this approach is very large. Indeed, this approach fails to track the desired attitude because the noises from motion accelerations affect the accelerometer data. Hence, the obtained results show that the CSMO is an efficient method for improving the attitude estimation quality.

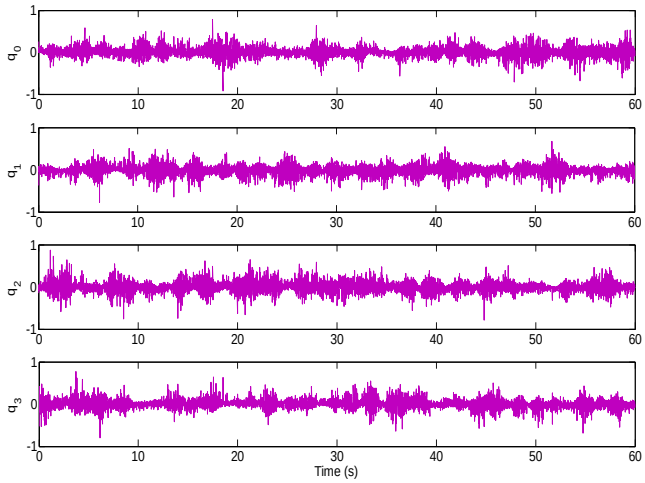

Fig. 7. Quaternion estimation errors using the Levenberg Marquardt Algorithm

VI. Experimental Validation

In order to evaluate the efficiency of the proposed CSMO in real world applications, an experimental setup was developed resorting to an inertial and magnetic sensor assembly. The goal is to obtain an estimation of the quaternion that represents the orientation of a rigid body and to investigate its accuracy under various conditions. For the experiments, two Inertial Measurement Units (IMUs) were employed: the *MTi* and the *MTi-G* from Xsens Motion Technologies [36] which output data at a rate of 100Hz (see Fig. 8).

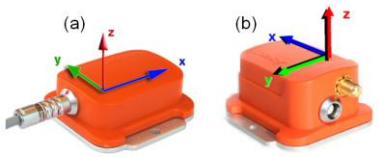

Fig. 8. IMUs with the sensor-fixed co-ordinate system - (a) *MTi* - (b) *MTi-G*

Those MEMS devices are a miniature, light weight, 3D calibrated digital output sensor (3D acceleration from accelerometer, 3D angular rate from gyroscope, and 3D magnetic field data from magnetometer) with built-in bias, sensitivity, and temperature compensation. Note that the *MTi-G* is a GPS enhanced Attitude and Heading Reference System (AHRS). In addition, these two devices are designed to track the body 3-D attitude output in quaternion representation. The calibration procedure to obtain the gains, offsets and non-orthogonality of the 3-axis accelerometer, the 3-axis gyroscope and the 3-axis magnetometer was performed by the manufacturer of the sensor module. More details about the sensor data specifications in these two devices are given in appendix C.

The *MTi* and the *MTi-G* can compute the attitude in quaternion representation by a traditional Kalman Filter (KF) and an Extended Kalman Filter (EKF), respectively, [36]. These algorithms exploit measurements from the inertial/magnetic sensors and GPS data (the GPS is only for the *MTi-G*). It is important to note that MT devices serve as tools for the evaluation of the Sliding Mode Observer efficiency and cannot be suitable for use in the field of ambulatory monitoring of human body motion and rehabilitation due to their dependences on an energy source as well as their heavy weights. In the following set of experiments, the calibrated data from the *MTi* and the *MTi-G* are used as input to the CSMO.

A. Robot mounted tests

In this section, the first experiment is achieved at the robotic laboratory of PSA Peugeot Citroën industrial base (Metz, France) under a popular industrial robot manipulator IRB 2400 from ABB Group [37]. It offers an excellent motion control around six axes and gives a high performance in the material handling with a position repeatability of 0.06mm and 0.1°. Note that to avoid considering the results provided by the *MTi* as a reference for the attitude measurement, some tests are performed by considering PSA's manipulator robot whose attitude and position are know exactly.

Before starting the experiment, the *MTi* was attached to a wooden board and joined to the last axis of the robot. A lot of attention is given during the assembly to obtain the two aligned frames *TooL0* and *T_st_iner* corresponding to the *MTi* and the last axis of the robot, respectively, (see Fig. 9). The reason is to get a ground truth orientation reference from the robot and to test the behavior of the inertial tracking approach. Notice that the length of the board is fixed to 20cm in order to place the unit far from the magnetic disturbance.

The ABB robot axes are programmed to rotate in such way of performing a trajectory like a straight line by the last axis in the space and without changing its orientation. Since the two frames are aligned, the *MTi* describes also the same attitude as

done by the robot axis. This motion is repeated many times by the robot to investigate the accuracy of the proposed filtering approach. During the experiment, we choose to increase the robot velocity at each test. The recorded data (angular rates, accelerations, Earth's magnetic fields) by the *MTi* are transmitted to a computer via USB port. Note that the robot gives the orientation of the frame *TooL0* in quaternion form. In the last step, we feed the CSMO with the recorded data by the *MTi* to obtain an estimation of orientation and to compare it with the one given by the robot.

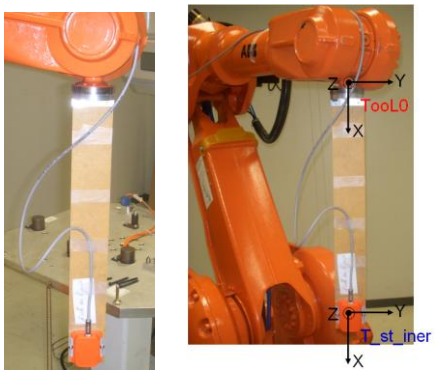

Fig. 9. Experimental setup: the *MTi* is mounted on the robot for orientation tracking

B. *Results and performances analysis*

Figures 10(a) and 11(a) show two series of the estimated quaternion components (orientation) by the proposed filtering algorithm for two different robot velocities. The goal is to verify if the proposed observer is disturbed by the change of the velocity rate. We can see that the observer estimates the truth attitude stably and smoothly.

We plotted also in the Figures 10(b) and 11(b) the corresponding residue after observer convergence, i.e., error between the CSMO and the reference (robot) for the quaternion components during the motion. This error is computed as the difference between the quaternion estimate produced by the CSMO and the robot. Note that this error is very small for the four quaternion components which proves the efficiency of the CSMO.

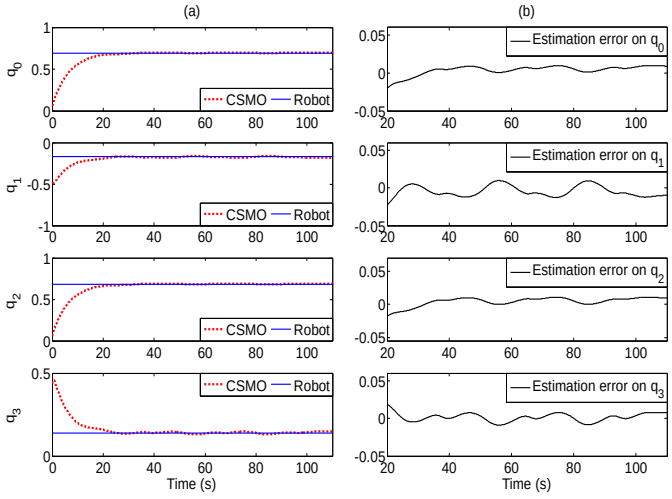

Fig. 10. (a) Comparison between quaternion components estimated from the CSMO and those given by the robot - (b) Quaternion estimation errors

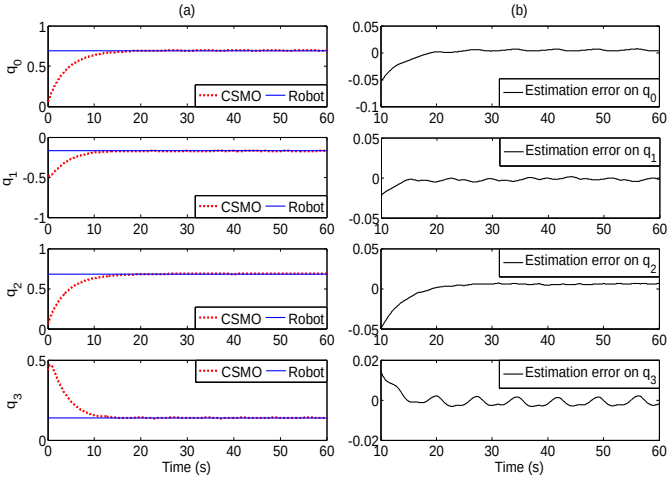

Fig. 11. Comparison between quaternion components estimated from the CSMO and those given by the robot - (b) Quaternion estimation errors

C. *Human motion segments evaluation*

An experimental trial was designed to evaluate the human body motion of one subject by comparing the orientations obtained using the proposed observer in (11) with those as determined using the *MTi-G* [36]. To validate the effectiveness of the CSMO, the experiments were chosen to cover a wide part of 3D human motion. Then, the subject was asked to perform the 4 exercises outlined in Fig. 12. So, the investigated experiments are carried out on the followings human segments: The foot segment (Fig. 12. (a)), the lower leg segment (Fig. 12. (b)), the upper arm (Fig. 12. (c)) and the head (Fig. 12. (d)). In each exercise, the *MTi-G* was attached to the segment using an adhesive tape. In the first exercise, the subject performed many tasks as toe rise foot, clockwise ankle rotation, lateral foot rotation and eversion (see Fig. 13). In the second exercise, firstly the subject makes an extension of the knee and secondly he rotates its leg in clockwise and anti-clockwise (see Fig. 14). The third exercise consists of the shoulder rotation, rotation around the axis defined along the upper arm and random motion (see Fig. 15). We finish this set of exercises with one performed on the head. The subject moves the neck firstly in two directions (clockwise and anti-clockwise. After, he makes a rotation around the lateral axis of the head and the exercise is finished by a random motion (see Fig. 16).

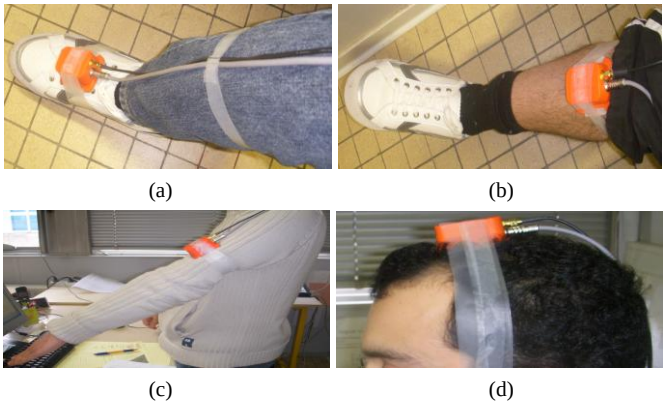

Fig. 12. Attachment of the *MTi-G* to the human limbs - (a) The foot segment - (b) The lower leg segment - (c) The upper arm - (d) The head

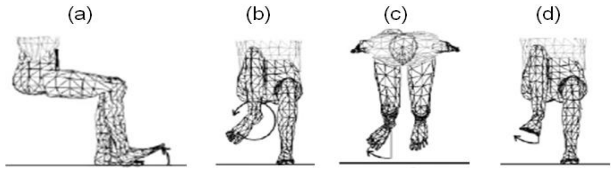

Fig. 13. Exercises performed during the foot segment motion - (a) Toe rise foot - (b) Clockwise ankle rotation - (c) Lateral foot rotation - (d) Eversion

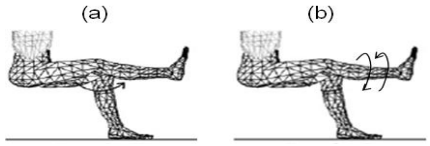

Fig. 14. Exercises performed during the lower leg segment motion - (a) Knee extension - (b) Clockwise and anti-clockwise rotation

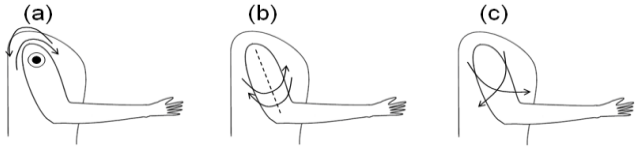

Fig. 15. Exercises performed during the upper arm motion - (a) clockwise and anti-clockwise shoulder rotation - (b) clockwise and anti-clockwise rotation around the dashed line axis defined along the upper arm segment - (c) random motion

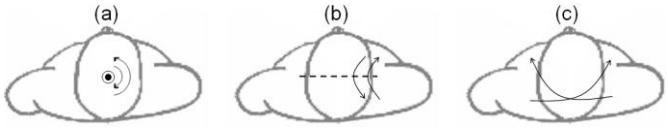

Fig. 16. Exercises performed during the head motion - (a) clockwise and anti-clockwise neck rotation - (b) clockwise and anti-clockwise rotation around dashed line lateral axis of the head - (c) random motion

The range of movement over which the technique was evaluated was large and comprehensive. Note that we have conducted several tests of these 4 exercises and that estimation results obtained were very similar. Therefore, we have chosen thereafter to represent only one illustrative example. During this experiment, the *MTi-G* recorded inertial/magnetic measurements and the 3D-orientation as a quaternion.

D. Results and performances analysis

The *Matlab* computing program was used for all post-trial data processing and analysis. The CSMO, proposed in section IV, is fed with calibrated data from the *MTi-G* to estimate the quaternion describing the orientation in each exercise. After that, the obtained estimations were compared to the orientations as determined using the *MTi-G*. In this section, we have chosen to represent the human motions orientation rather in Euler angles representation (roll, pitch and yaw) because it is more intuitive than quaternion for the reader. The mathematical transformation between quaternion and Euler angles is given in [38].

Figures 17(a), 18(a), 19(a) and 20(a) show the time history evolution of the Euler angles obtained from the *MTi-G* and the CSMO. These figures represent the foot, lower leg, upper arm and head motions, respectively. Thus, one can deduce a strong correlation between the orientations measured using the *MTi-G* and the CSMO. Note that the convergence rate is very fast and is around 2 sec. The roll, pitch and yaw estimation errors are shown also in the Figures 17(b), 18(b), 19(b) and 20(b) to provide an overview of the overall performance of the proposed approach in the paper. These errors are computed as the difference between Euler angles estimates produced by the CSMO and the *MTi-G*.

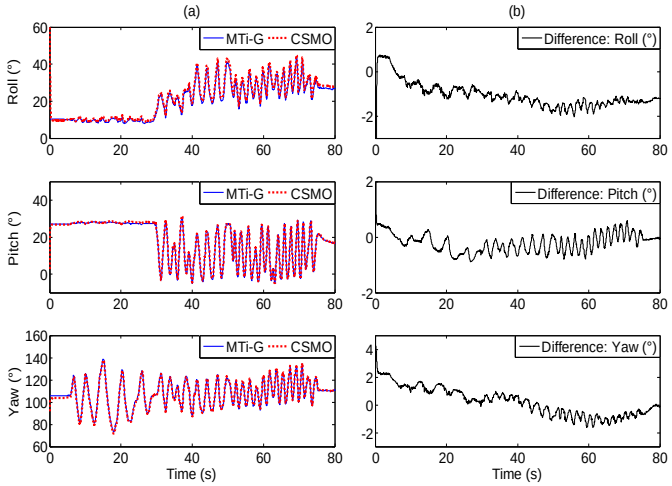

Fig. 17. (a) Comparison of Euler angles estimated from the CSMO and those obtained by *MTi-G* - (b) The corresponding estimation errors (Exercise on the foot segment)

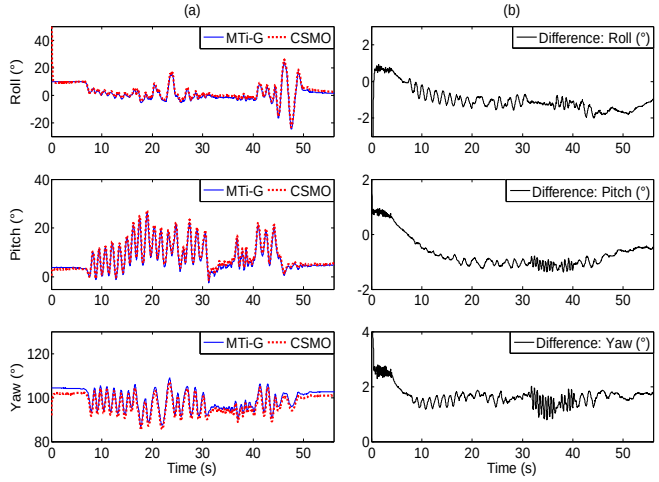

Fig. 18. (a) Comparison of Euler angles estimated from the CSMO and those obtained by the *MTi-G* - (b) The corresponding estimation errors (Exercise on the lower leg segment)

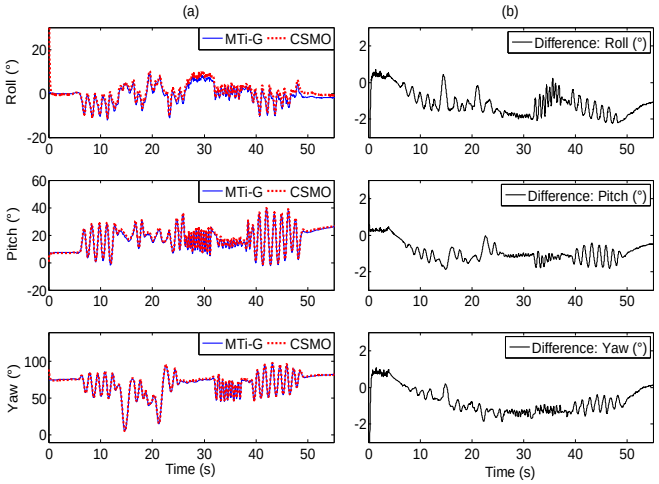

Fig. 19. (a) Comparison of Euler angles estimated from the CSMO and those obtained by the *MTi-G* - (b) The corresponding estimation errors (Exercise on the upper arm)

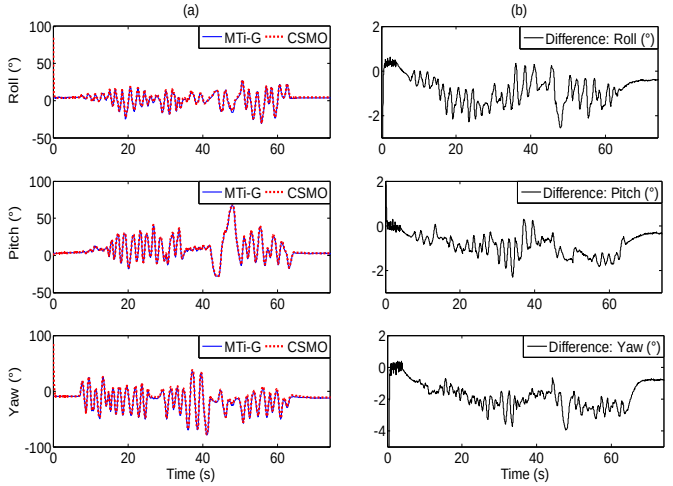

Fig. 20. (a) Comparison of Euler angles estimated from the CSMO and those obtained by the *MTi-G* - (b) The corresponding estimation errors (Exercise on the head)

The performance level consistency of the observer may be illustrated in these figures, even in dynamic situations, since the estimation errors are very small (around 2° for roll and pitch angles and 3° for yaw angle). It is important to note that although **our approach didn't exploit the GPS data** as the internal algorithm of the *MTi-G*, it is able to reconstruct the orientation of the hand (given by the *MTi-G*) with a small error. Note that, we have already shown experimentally in [19] that the results provided by the *MTi* algorithms (Kalman Filter) in estimating orientation suffer from lack of robustness mainly during the dynamic motion (high inertial acceleration a).

The observer performance is shown quantitatively using the Root Mean Square Error (RMSE) of Euler angles measured by the CSMO when compared with the angles measured by the *MTi-G*. The RMSE was calculated as shown below [21]:

$$RMSE = \sqrt{\frac{\sum_{k=1}^{T}\left(A_s(k) - \hat{A}_s(k)\right)^2}{T}} \qquad (23)$$

where

s : The exercise that was chosen.

A_s : The Euler angle being measured by the *MTi-G*.

$\hat{A}_s$: The Euler angle being estimated by the CSMO.

T : The time interval chosen as $T = 2$.

In Figures 21, 22 and 23, the distribution of the RMSEs of Euler angles (Fig. 21 for the roll angle, Fig. 22 for the pitch angle, and Fig. 23 for the yaw angle) is presented in box plots. These RMSEs are defined using the CSMO method when compared with the Euler angles measured by the *MTi-G* for each exercise. The tops and bottoms of each box are the 25th and 75th percentiles of the samples, respectively. The distances between the tops and bottoms of the boxes are the inter-quartile ranges (IQR). The horizontal lines in the middle of each box illustrate median values. The whiskers are lines extending above and below each box. Whiskers are drawn from the ends of the inter-quartile ranges to the furthest observations within the whisker length (the adjacent values). Observations beyond the whisker length are marked as outliers. By default, an outlier is a value that is more than 1.5 times the inter-quartile range away from the top or bottom of the box. Outliers are displayed with a red (+) sign.

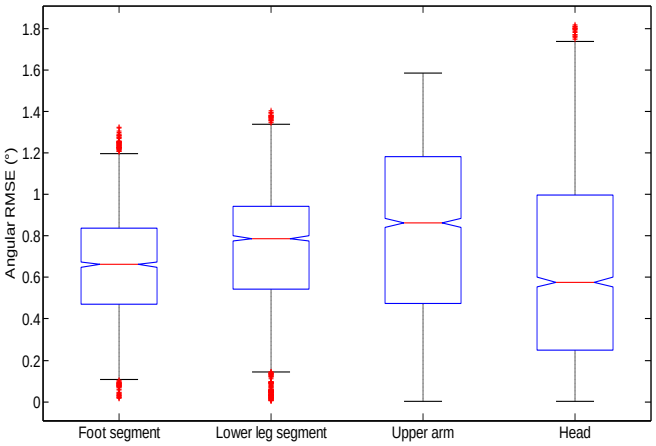

Fig. 21. Box plot of the RMSEs in degrees of the roll angle estimated by the CSMO when compared with the roll angle measured by the *MTi-G*

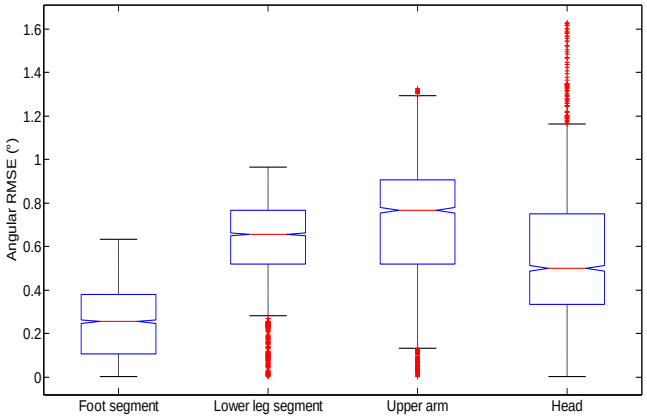

Fig. 22. Box plot of the RMSEs in degrees of the pitch angle estimated by the CSMO when compared with the pitch angle measured by the *MTi-G*

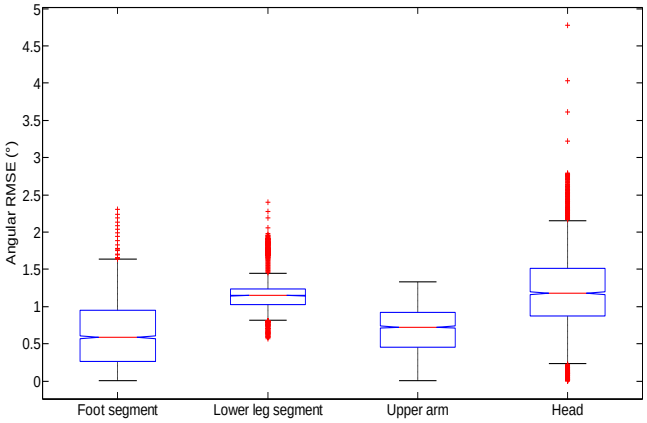

Fig. 23. Box plot of the RMSEs in degrees of the yaw angle estimated by the CSMO when compared with the yaw angle measured by the *MTi-G*

The statistics from these figures are grouped in Tables III, IV, and V for roll, pitch and yaw angles, respectively. These Tables show that the RMSE and IRQ values are so small for each exercise. Therefore, we can conclude that accurate measurements of human body segment orientation can be achieved by the proposed technique based on the CSMO during a variety of human motion exercises.

TABLE III
RMSES (MEDIAN) AND IRQS OF ROLL ANGLE FOR EACH EXERCISE

	Foot segment	Lower leg segment	Upper arm	Head
RMSEs (median)	0.661	0.787	0.862	0.577
IQR	0.366	0.398	0.706	0.750

TABLE IV
RMSES (MEDIAN) AND IRQS OF PITCH ANGLE FOR EACH EXERCISE

	Foot segment	Lower leg segment	Upper arm	Head
RMSEs (median)	0.254	0.655	0.766	0.500
IQR	0.272	0.247	0.387	0.413

TABLE V
RMSES (MEDIAN) AND IRQS OF YAW ANGLE FOR EACH EXERCISE

	Foot segment	Lower leg segment	Upper arm	Head
RMSEs (median)	0.586	1.146	0.721	1.177
IQR	0.686	0.214	0.561	0.642

VII. CONCLUSION

This paper proposes a quaternion-based Complementary Sliding Mode Observer approach (CSMO) to recover the human body segments motions with a set of MEMS inertial and magnetic sensors. The suggested applications are for human motion monitoring and analysis in rehabilitation and sport medicine. The CSMO exploits readings with a view to do a trade-off between a good short term precision given by rate gyros integration and a reliable long term accuracy provided by accelerometer and magnetometer measurements. This alternative approach combines the kinematic equation of a rigid body with the Levenberg Marquardt Algorithm (LMA) that combines Earth's magnetic field and gravity's vector. The efficiency of the approach herein designed is demonstrated through some simulations using a theoretical example. Moreover, some experiments are carried out on a robot manipulator and some human body segments through sensor measurements provided by an Inertial Measurement Unit. The obtained results illustrate the performance of the proposed approach to estimate the main human movements with small errors.

Future works will be focused on the application of the proposed approach firstly in the online ambulatory monitoring of human body motion for the elderly to prevent injuries or detect falls of persons for example.

APPENDIX

A. Quaternion algebra

The unit quaternion, denoted by q, is expressed as:

$$q = q_0 + q_{vect} = q_0 + q_1 i + q_2 j + q_3 k \in Q \quad (24)$$

where $q_{vect} = q_1 i + q_2 j + q_3 k$ represents the imaginary vector, and q_0 is the scalar element.

The quaternion product of $q_a = \begin{bmatrix} q_{a0} & q_{a,vect}^T \end{bmatrix}^T$ and $q_b = \begin{bmatrix} q_{b0} & q_{b,vect}^T \end{bmatrix}^T$ is defined such as:

$$q_a \otimes q_b = \begin{bmatrix} q_{a0} & -q_{a,vect}^T \\ q_{a,vect} & I_{3\times3} q_{a0} + \begin{bmatrix} q_{a,vect}^\times \end{bmatrix} \end{bmatrix} \begin{bmatrix} q_{b0} \\ q_{b,vect} \end{bmatrix} \quad (25)$$

where $I_{3\times3}$ is the identity matrix and $\begin{bmatrix} q_{a,vect}^\times \end{bmatrix}$ represents the standard vector cross-product which is defined as [7]:

$$\begin{bmatrix} q_{a,vect}^\times \end{bmatrix} = \begin{bmatrix} 0 & -q_{a3} & q_{a2} \\ q_{a3} & 0 & -q_{a1} \\ -q_{a2} & q_{a1} & 0 \end{bmatrix} \quad (26)$$

We invite the reader to refer to [31] for a more details about quaternion algebra.

B. Main frames for attitude definition

The attitude estimation requires the transformation of measured and computed quantities between various frames. The attitude of a rigid body is based on measurements gained from sensors attached to it. Indeed, inertial sensors are attached to the body-platform and provide measurements expressed relative to the instrument axes. In most systems, the instrument axes are nominally aligned with the body-platform axes. Since the measurements are performed in the body frame, we describe in Fig. 24 the orientation of the body-fixed frame $B(X_B, Y_B, Z_B)$ with respect to the Earth-fixed frame $N(X_N, Y_N, Z_N)$ which is tangent to the Earth's surface.

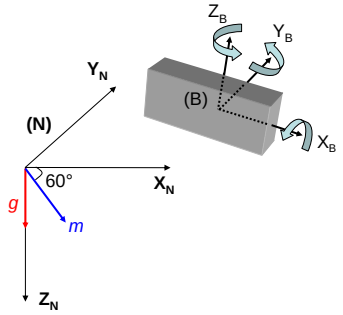

Fig. 24. The coordinate system (*B*) of a rigid body represented in the Earth-fixed frame (*N*)

This local coordinate is particularly useful to express the attitude of a moving rigid body on the surface of the earth [17]. The X_N-axis points true north. The Z_N-axis points towards the interior of the Earth, perpendicular to the reference ellipsoid. The Y_N-axis completes the right-handed coordinate system, pointing east (NED: North, East, Down).

C. MTi and MTi-G performances

We show in the Table VI the performances of the MT Devices (*MTi* and *MTi-G*) [38].

TABLE VI
CALIBRATED DATA PERFORMANCE SPECIFICATION OF THE MT DEVICES

Sensor performance	Rate of turn	Acceleration	Magnetic field
Full scale	± 300 deg/s	± 50 m/s^2	± 750 mGauss
Bias stability	1 deg/s	0.02 m/s^2	0.1 mGauss
Noise	0.05 deg/s/$\sqrt{\text{Hz}}$	0.002 m/s^2/$\sqrt{\text{Hz}}$	0.5 mGauss
Alignment error	0.1 deg	0.1 deg	0.1 deg

ACKNOWLEDGMENT

The authors would like to thank both the Alsace and Champagne-Ardenne regions (France) within the framework of the project (NaviMeles) for their financial support. Also, we gratefully acknowledge Mr. Pierre Seger from the robotic laboratory of PSA Peugeot Citroën industrial base (Metz, France) for his help during the robot experiments.

REFERENCES

[1] H. Zhou and H. Hu, "Human motion tracking for rehabilitation-A survey," *Biomedical Signal Processing and control*, vol. 3, no. 1, pp. 1-18, January 2008.

[2] H. Zhou, H. Hu, N. D. Harris, and J. Hammerton, "Applications of wearable inertial sensors in estimation of upper limb movements," *Biomedical Signal Processing and control*, vol. 1, no. 1, pp. 22-32, January 2006.

[3] A. M. Sabatini, "Quaternion-based strap-down integration method for applications of inertial sensing to gait analysis," *Medical & Biological Engineering & Computing*, vol. 43, no. 1, pp. 94-101, January 2005.

[4] M. J. Mathie, A. C. F. Coster, N. H. Lovell, and B. G. Celler, "Detection of daily physical activities using a triaxial accelerometer," *Medical and Biological Engineering Computing*, vol. 41, no. 3, pp. 296-301, May 2003.

[5] P. H. Veltink, "Sensory feedback in artificial control of human mobility," *Technology and Health Care archive*, vol. 7, no. 6, pp. 383-391, January 1999.

[6] C. Verplaeste, "Inertial proprioceptive devices: self-motion-sensing toys and tools," *IBM Systems Journal*, vol. 35, no. 3-4, pp. 639-650, 1996.

[7] K. Parsa, Ty A. Lasky, and B. Ravani, "Design and Implementation of a Mechatronic, All-Accelerometer Inertial Measurement Unit," *IEEE/ASME Transactions on Mechatronics*, vol. 12, no. 6, pp. 640-650, December 2007.

[8] H. J. Luinge and P. H. Veltink, "Inclination measurement of human movement using a 3-D accelerometer with autocalibration," *IEEE Transactions on Neural Systems and Rehabilitation Engineering*, vol. 12, no. 1, pp. 112-121, March 2004.

[9] J. E. Bortz, "A new mathematical formulation for strap-down inertial navigation," *IEEE Transactions on Aerospace and Electronic Systems*, vol. 7, no. 1, pp. 61-66, January 1971.

[10] M. J. Caruso, "Applications of magnetic sensors for low cost compass systems," *IEEE Position, Location and Navigation Symposium*, San Diego, CA, 2000, pp. 177-184.

[11] B. Kemp, A. J. M. W. Janssen, and B. Van der Kamp, "Body position can be monitored in 3D using miniature accelerometers and earth magnetic field sensors," *Electroencephalography and Clinical Neurophysiology/Electromyography and Motor Control*, vol. 109, no. 6, pp. 484-488, December 1998.

[12] H. J. Luinge and P. H. Veltink, "Measuring orientation of human body segments using miniature gyroscopes and accelerometers," *Medical and Biological Engineering and Computing*, vol. 43, no. 2, pp. 273-282, 2005.

[13] R. Zhu and Z. Zhou, "A real-time articulated human motion tracking using tri-axis inertial/magnetic sensors package," *IEEE Transactions on Neural Systems and Rehabilitation Engineering*, vol. 12, no. 2, pp. 295-302, June 2004.

[14] D. Roetenberg, H. J. Luinge, C. T. M. Baten, and P. H. Veltink, "Compensation of magnetic disturbances improves inertial and magnetic sensing of human body segment orientation," *IEEE Transactions on Neural Systems and Rehabilitation Engineering*, vol. 13, no. 3, pp. 395-405, September 2005.

[15] A. M. Sabatini, "Quaternion-based Extended Kalman Filter for determining orientation by inertial and magnetic sensing," *IEEE Transactions on Biomedical Engineering*, vol. 53, no. 7, pp. 1346-1356, July 2006.

[16] D. Roetenberg, P. J. Slycke, and P. H. Veltink, "Ambulatory position and orientation tracking fusing magnetic and inertial sensing," *IEEE Transactions on Biomedical Engineering*, vol. 54, no. 5, pp. 883-890, May 2007.

[17] R. Mahony, T. Hamel, and J. M. Pflimlin, "Nonlinear complementary filters on the special orthogonal group,", *IEEE Transactions on Automatic Control*, vol. 53, no. 5, pp. 1203-1218, June 2008.

[18] V. Van Acht, E. Bongers, N. Lambert, and R. Verberne, "Miniature Wireless Inertial Sensor for Measuring Human Motions," *29th Annual International Conference of the IEEE EMBS*, Lyon, France, 2007, pp. 6278-6281.

[19] H. Fourati, N. Manamanni, L. Afilal, and Y. Handrich, "Nonlinear Filtering Approach for the Attitude and Dynamic Body Acceleration Estimation Based on Inertial and Magnetic Sensors: Bio-logging Application (Periodical style-Accepted for publication)," *IEEE Sensors Journal*, 2010, to be published, doi: 10.1109/JSEN.2010.2053353.

[20] R.G. Brown and P.Y.C Hwang, *Introduction to Random Signal and Applied Kalman Filtering*, 3rd Ed. New York: John Wiley, 1997.

[21] A. U. Alahakone and S. M. N. Arosha Senanayake, "A Real-Time System With Assistive Feedback for Postural Control in Rehabilitation," *IEEE/ASME Transactions on Mechatronics*, vol. 15, no. 2, pp. 226-233, April 2010.

[22] S. Beeby, G. Ensell, M. Kraft, and N. White, *MEMS Mechanical Sensors*, Artech House House Publishers, 2004.

[23] M. D. Shuster, "A survey of attitude representations," *Journal of the Astronautical Science*, vol. 41, no. 4, pp. 493-517, October-December 1993.

[24] H. Fourati, N. Manamanni, L. Afilal, and Y. Handrich, "Posture and body acceleration tracking by inertial and magnetic sensing: Application in behavioral analysis of free-ranging animals (Periodical style-Accepted for publication)," *Biomedical Signal Processing and Control*, 2010, to be published, doi: 10.1016/j.bspc.2010.06.004.

[25] G. Wahba, "A least squares estimate of spacecraft attitude," *SIAM, Review*, vol. 7, no. 3, pp. 409, July 1965.

[26] Astrosurf, (2010, January). Available: http://www.astrosurf.com.

[27] W. Wang and O. A. Jianu, "A Smart Sensing Unit for Vibration Measurement and Monitoring," *IEEE/ASME Transactions on Mechatronics*, vol. 15, no. 1, pp. 70-78, February 2010.

[28] H. Fourati, N. Manamanni, L. Afilal, and Y. Handrich, "A quaternion-based Complementary Sliding Mode Observer for attitude estimation: application in free-ranging animal motions," *49th IEEE Conference on Decision and Control (CDC)*, Atlanta, USA, December 2010.

[29] J. E. Dennis, Jr. and Robert B. Schnabel, *Numerical Methods for Unconstrained Optimization and Nonlinear Equations*, Prentice Hall, Englewood, NJ, 1983.

[30] H. Fourati, N. Manamanni, L. Afilal, and Y. Handrich, "Sensing technique of dynamic marine animal's attitude by use of low-cost inertial and magnetic sensors," *8th IFAC Conference on Control Applications in Marine Systems (CAMS)*, Rostock-Warnemünde, Germany, 2010, pp. 318-323.

[31] J. B. Kuipers, *Quaternion and Rotation Sequences*, Princeton, NJ: Princeton University Press, 1999.

[32] J. J. E. Slotine, J. K. Hedrick, and A. Misawa, A, "On sliding Observers for Nonlinear Systems," *ASME Journal of Dynamic Systems, Measurement and Control*, vol. 109, pp. 245-252, 1987.

[33] J. Deutschmann, I. Bar-Itzhack, and K. Galal, "Quaternion normalization in spacecraft attitude determination," *AIAA Astrodynamics Conference*, Washington, USA, 1992, pp. 27-37.

[34] H. Fourati, N. Manamanni, L. Afilal, and Y. Handrich, "A rigid body attitude estimation for Bio-logging application: A quaternion-based nonlinear filter approach," *IEEE/RSJ International conference on Intelligent Robots and Systems IROS'09*, St. Louis, USA, 2009, pp. 558-563.

[35] W. Higgins, "A comparison of complementary and Kalman filtering," *IEEE Transactions on Aerospace and Electronic Systems*, vol. 11, no. 3, pp. 321-325, May 1975.

[36] Xsens Motion Technologies, (2010, September). Available: http://www.xsens.com.

[37] ABB Group. (2010, September). Available: http://www.abb.com.

[38] W. F. Phillips, C. E. Hailey, and G. A. Gebert, "Review of attitude representations used for aircraft kinematics," *Journal of Aircraft*, vol. 38, no. 4, pp. 718-223 , July-August 2001.